Article

Using Physical Chemistry To Differentiate Nicotinic from Cholinergic Agonists at the Nicotinic Acetylcholine Receptor

Amanda L. Cashin, E. James Petersson, Henry A. Lester, and Dennis A. Dougherty

J. Am. Chem. Soc., **2005**, 127 (1), 350-356• DOI: 10.1021/ja0461771 • Publication Date (Web): 02 December 2004

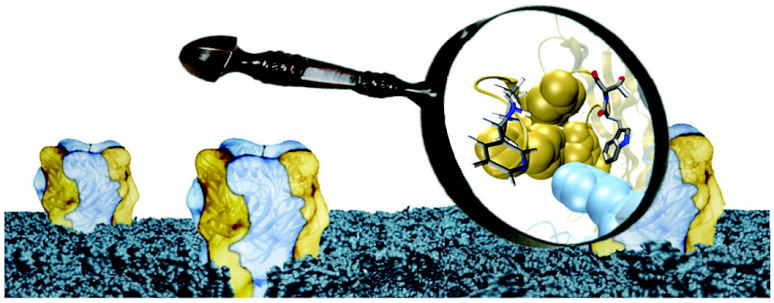

J|A|C|S
ARTICLES
Published on Web 12/02/2004

Using Physical Chemistry To Differentiate Nicotinic from Cholinergic Agonists at the Nicotinic Acetylcholine Receptor

Amanda L. Cashin,[†] E. James Petersson,[†] Henry A. Lester,[‡] and Dennis A. Dougherty*,[†]

Contribution from the Division of Chemistry and Chemical Engineering and Division of Biology, California Institute of Technology, 1200 East California Boulevard, Pasadena, California 91125

Received June 28, 2004; E-mail: dadougherty@caltech.edu

Abstract: The binding of three distinct agonists—acetylcholine (ACh), nicotine, and epibatidine—to the nicotinic acetylcholine receptor has been probed using unnatural amino acid mutagenesis. ACh makes a cation−π interaction with Trp α149, while nicotine employs a hydrogen bond to a backbone carbonyl in the same region of the agonist binding site. The nicotine analogue epibatidine achieves its high potency by taking advantage of both the cation−π interaction and the backbone hydrogen bond. A simple structural model that considers only possible interactions with Trp α149 suggests that a novel aromatic C−H···O=C hydrogen bond further augments the binding of epibatidine. These studies illustrate the subtleties and complexities of the interactions between drugs and membrane receptors and establish a paradigm for obtaining detailed structural information.

Introduction

Biological signaling pathways employ a vast array of integral membrane proteins that process and interpret the chemical, electrical, and mechanical signals that are delivered to cells. These receptor/channel proteins are the targets of most drugs of therapy and abuse, but structural insights are sparse because both X-ray crystallography and NMR spectroscopy are of limited applicability. Even when structural information is available, establishing the functional importance of particular structural features can be challenging. In contrast, chemistry-based methods hold great promise for producing high-precision structural and functional insights. Varying the drug or signaling molecule has been the approach of the pharmaceutical industry, producing a multitude of structure−activity relationships of considerable value. In recent years we have taken the reverse approach, in which we systematically vary the receptor and use functional assays to monitor changes in drug−receptor interactions.[1,2] We show here that this physical chemistry approach to studying receptors can produce high-precision insights into drug−receptor interactions. In particular, we show that two agonists that interact with the same binding pocket of a receptor can make use of very different noncovalent interactions to achieve the same result.

The ligand gated ion channels (LGIC) are among the molecules of memory, thought, and sensory perception and are the targets for treatments of Alzheimer's disease, Parkinson's disease, schizophrenia, stroke, learning deficits, and drug addiction.[3] The binding of small-molecule neurotransmitters induces a structural change, opening a pore in a channel that allows the passage of ions across the cell membrane. Here we examine the agonist-binding site of the nicotinic acetylcholine receptor (nAChR), the prototype of the Cys-loop family of LGIC, which also includes γ-aminobutyric acid, glycine, and serotonin receptors. The embryonic muscle nAChR is a cylindrical transmembrane protein[4] composed of five subunits, $(\alpha 1)_2$, $\beta 1$, γ, and δ (Figure 1A). Early biochemical studies identified two agonist binding sites localized to the α/δ and α/γ interfaces.[5−7] The crystal structure of the acetylcholine

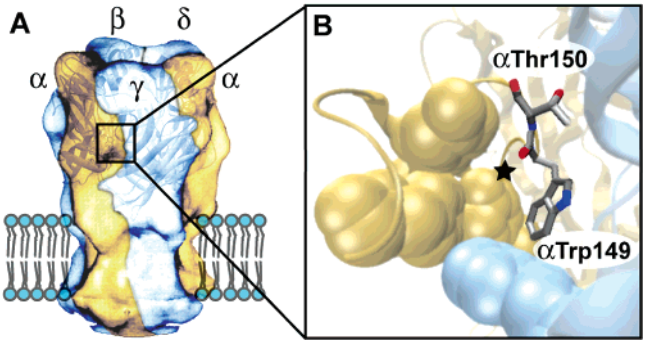

Figure 1. Images of the nAChR. (A) The overall layout of the muscle receptor, indicating the arrangement of five subunits around a central pore. The receptor electron density from cryoelectron microscopy[4] is shown superimposed over a ribbon diagram of AChBP,[8] which corresponds to the extracellular domain of the receptor. (B) The agonist binding site from AChBP with muscle-type nAChR numbering. Aromatic residues lining the binding pocket are shown as space-filling models. Residues and ribbons from the α subunit are gold; those from the δ subunit are blue. The star marks the backbone carbonyl that participates in a hydrogen bond with agonists.

[†] Division of Chemistry and Chemical Engineering.
[‡] Division of Biology.

(1) Beene, D. L.; Dougherty, D. A.; Lester, H. A. *Curr. Opin. Neurobiol.* **2003**, *13*, 264−270.
(2) Dougherty, D. A. *Curr. Opin. Chem. Biol.* **2000**, *4*, 645−652.
(3) Paterson, D.; Nordberg, A. *Prog. Neurobiol.* **2000**, *61*, 75−111.
(4) Miyazawa, A.; Fujiyoshi, Y.; Stowell, M.; Unwin, N. *J. Mol. Biol.* **1999**, *288*, 765−786.

10.1021/ja0461771 CCC: $30.25

binding protein (AChBP),[8] a soluble protein homologous to the agonist binding site of the nAChR, revealed the binding sites to be defined by a box of conserved aromatic residues.

A cationic center is contained in nearly all nAChR agonists, including acetylcholine (ACh) and (−)-nicotine. A common strategy for the recognition of cations by biological molecules uses the cation−π interaction, the stabilizing interaction between a cation and the electron-rich face of an aromatic ring.[9−11] Studies of the muscle-type nAChR using unnatural amino acid mutagenesis showed that a key tryptophan, Trp α149, makes a potent cation−π interaction with ACh in the agonist binding site.[12] Interestingly, nicotine binding in the same pocket of the muscle-type nAChR does not make a strong cation−π interaction.[13] These findings suggested that agonists of the nAChR could fall into two classes, which for present purposes we will term "cholinergic", binding like ACh, and "nicotinic", binding like nicotine.

Several modeling studies based on the original structure of AChBP suggested a hydrogen-bonding interaction from the $N^+-\mathbf{H}$ of nicotine to the backbone carbonyl of Trp α149.[14,15] This carbonyl is denoted by a star in Figure 1. ACh cannot make a hydrogen bond of this sort. Thus, this hydrogen bond could be a second discriminator between ACh and nicotine (the first being the cation−π interaction with Trp α149). While this work was nearing completion, Sixma and co-workers reported the crystal structure of AChBP in the presence of bound nicotine,[16] confirming the proposed hydrogen bond between nicotine and the backbone carbonyl of Trp α149 at the agonist-binding site. We note, however, that AChBP is not a neuroreceptor, and that it shares only 20−24% sequence identity with nAChR α subunits. In addition, the crystal structure of AChBP most likely represents the desensitized state of the receptor. Thus, the *functional* significance of structural insights gained from AChBP remains to be determined, and the present paper addresses this issue.

One challenge in studying the activity of nicotine at the nAChR is that nicotine has low agonist potency at the muscle receptor subtype.[17] Nicotine is a more potent agonist at some neuronal nAChR subtypes.[18] As such, the present study also examines epibatidine, a very potent agonist at both muscle- and neuronal-type nAChRs.[18,19] Epibatidine, while structurally similar to nicotine, has a potency comparable to that of ACh.[20,21]

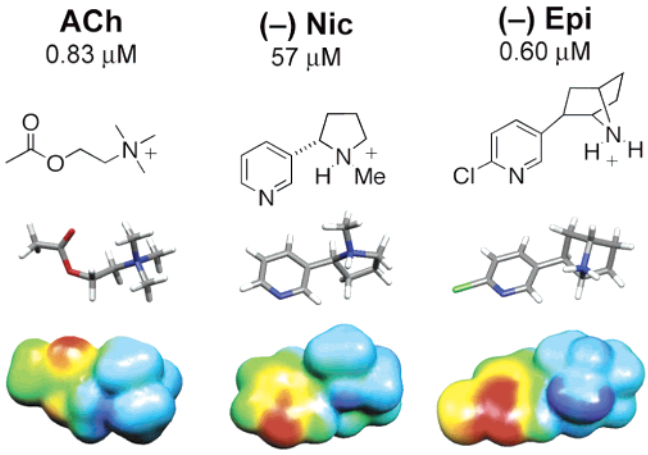

Figure 2. nAChR agonists examined in this study. Shown are EC_{50} values for activation of the wild-type nAChR and calculated agonist geometries. HF/6-31G electrostatic surfaces calculated using Molekel contrast the focused $N^+-\mathbf{H}$ positive charge on nicotine and epibatidine with the diffuse ACh ammonium charge. Electrostatic surfaces correspond to an energy range of +10 to +130 kcal/mol, where blue is highly positive and red is less positive. Note that (±)-epibatidine was used to obtain EC_{50} values.

Therefore, epibatidine perhaps serves as a more meaningful probe of "nicotinic" interactions at the muscle-type nAChR (Figure 2).

The goals of this study were thus two-fold. First, we wished to evaluate the significance of the apparent hydrogen bond between nicotine and the backbone carbonyl of Trp α149. Second, we wished to evaluate the factors that render epibatidine almost 100-fold more potent than nicotine, despite the clear structural similarity of the two. The site-specific in vivo nonsense suppression methodology for unnatural amino acid incorporation[2] has been exploited to evaluate these two issues. Studies employing fluorinated Trp derivatives at α149 reveal that epibatidine binds with a potent cation−π interaction similar to that of ACh. In addition, we establish the functional significance of the interaction with the backbone carbonyl at Trp α149 with both nicotine and epibatidine by weakening the hydrogen-bonding ability of the backbone carbonyl through an appropriate backbone amide-to-ester mutation. Modeling based on these data suggests precise interactions that differentiate the three agonists.

Materials and Methods

Preparation of α-Hydroxythreonine (Tah). α-Hydroxythreonine (Tah) (2*R*,3*S*-dihydroxybutanoate) cyanomethyl ester was synthesized according to previously published methods.[22,23] Detailed synthetic procedures are available in the Supporting Information.

Electrophysiology. Stage VI oocytes of *Xenopus laevis* were employed. Oocyte recordings were made 24−48 h after injection in two-electrode voltage clamp mode using the OpusXpress 6000A (Axon Instruments, Union City, CA). Oocytes were superfused with Ca^{2+}-free ND96 solution at flow rates of 1 and 4 mL/min during drug application and 3 mL/min during wash. Holding potentials were −60 mV. Data were sampled at 125 Hz and filtered at 50 Hz. Drug applications were 15 s in duration. Agonists were purchased from Sigma/Aldrich/RBI (St. Louis, MO): [(−)-nicotine tartrate, acetylcholine chloride, and (±)-epibatidine dihydrochloride]. Epibatidine was also purchased from Tocris (Ellisville, MO) [(±)-epibatidine]. All drugs

(5) Grutter, T.; Changeux, J. P. *Trends Biochem. Sci.* **2001**, *26*, 459−463.
(6) Karlin, A. *Nat. Rev. Neurosci.* **2002**, *3*, 102−114.
(7) Corringer, P.-J.; Le Novère, N.; Changeux, J.-P. *Annu. Rev. Pharmacol. Toxicol.* **2000**, *40*, 431−458.
(8) Brejc, K.; van Dijk, W. J.; Klaassen, R. V.; Schuurmans, M.; van Der Oost, J.; Smit, A. B.; Sixma, T. K. *Nature* **2001**, *411*, 269−276.
(9) Dougherty, D. A. *Science* **1996**, *271*, 163−168.
(10) Ma, J. C.; Dougherty, D. A. *Chem. Rev.* **1997**, *97*, 1303−1324.
(11) Zacharias, N.; Dougherty, D. A. *Trends Pharmacol. Sci.* **2002**, *23*, 281−287.
(12) Zhong, W.; Gallivan, J. P.; Zhang, Y.; Li, L.; Lester, H. A.; Dougherty, D. A. *Proc. Natl. Acad. Sci. U.S.A.* **1998**, *95*, 12088−12093.
(13) Beene, D. L.; Brandt, G. S.; Zhong, W.; Zacharias, N. M.; Lester, H. A.; Dougherty, D. A. *Biochemistry* **2002**, *41*, 10262−10269.
(14) Schapira, M.; Abagyan, R.; Totrov, M. *BMC Struct. Biol.* **2002**, *2*, 1.
(15) Le Novere, N.; Grutter, T.; Changeux, J. P. *Proc. Natl. Acad. Sci. U.S.A.* **2002**, *99*, 3210−3215.
(16) Celie, P. H. N.; van Rossum-Fikkert, S. E.; van Dijk, W. J.; Brejc, K.; Smit, A. B.; Sixma, T. K. *Neuron* **2004**, *41*, 907−914.
(17) Akk, G.; Auerbach, A. *Br. J. Pharmacol.* **1999**, *128*, 1467−1476.
(18) Gerzanich, V.; Peng, X.; Wang, F.; Wells, G.; Anand, R.; Fletcher, S.; Lindstrom, J. *Mol. Pharmacol.* **1995**, *48*, 774−782.
(19) Prince, R. J.; Sine, S. M. *Biophys. J.* **1998**, *75*, 1817−1827.
(20) Badio, B.; Daly, J. W. *Mol. Pharmacol.* **1994**, *45*, 563−569.
(21) Dukat, M.; Glennon, R. A. *Cell Mol. Neurobiol.* **2003**, *23*, 365−378.
(22) Servi, S. *J. Org. Chem.* **1985**, *50*, 5865−5867.
(23) England, P. M.; Lester, H. A.; Dougherty, D. A. *Tetrahedron Lett.* **1999**, *40*, 6189−6192.

were prepared in sterile distilled, deionized water for dilution into calcium-free ND96. Dose−response data were obtained for a minimum of 10 concentrations of agonists and for a minimum of 7 cells. Dose−response relations were fitted to the Hill equation to determine EC_{50} and the Hill coefficient. EC_{50} values for individual oocytes were averaged to obtain the reported values.

Unnatural Amino Acid Suppression. Synthetic amino acids and α-hydroxy acids were conjugated to the dinucleotide dCA and ligated to truncated 74 nt tRNA as previously described.[23,24] Deprotection of amino acyl tRNA was carried out by photolysis immediately prior to co-injection with mRNA, as described.[24,25] Typically, 25 ng of tRNA was injected per oocyte along with mRNA in a total volume of 50 nL/cell. mRNA was prepared by in vitro runoff transcription using the Ambion (Austin, TX) T7 mMessage mMachine kit. Mutation to the *amber* stop codon at the site of interest was accomplished by standard means and was verified by sequencing through both strands. For nAChR suppression, a total of 4.0 ng of mRNA was injected in the subunit ratio of 10:1:1:1 α:β:γ:δ. In all cases, the β subunit contained a Leu9′Ser mutation, as discussed below. Mouse muscle embryonic nAChR in the pAMV vector was used, as reported previously. In addition, the α subunits contain an HA epitope in the M3−M4 cytoplasmic loop for biochemical studies (data not shown). Control experiments show a negligible effect of this epitope on EC_{50}. As a negative control for suppression, truncated 74 nt or truncated tRNA ligated to dCA was co-injected with mRNA in the same manner as fully charged tRNA. At the positions studied here, no current was ever observed from these negative controls. The positive control for suppression involved wild-type recovery by co-injection with 74 nt tRNA ligated to dCA-Thr or dCA-Trp. In all cases, the dose−response data were indistinguishable from those for injection of wild-type mRNA alone.

Computation. Acetylcholine, (−)-nicotine, (+)-epibatidine, (−)-epibatidine, 3-(1*H*-indol-3-yl)-*N*-methylpropionamide, 3-(1*H*-indol-3-yl)-*O*-methylpropionate, and the hydrogen-bonded complexes shown in Figure 5 were optimized at the HF/6-31G level of theory. For the acetylcholine, (−)-nicotine, and (−)-epibatidine complexes, the starting coordinates of the ligand and Trp 147 (α7 numbering) were taken from the docked structures of LeNovere and Changeux, available at http://www.ebi.ac.uk/compneur-srv/LGICdb/LGIC.html. The optimized geometries were fully characterized as minima by frequency analysis and are reported in the Supporting Information. Energies were calculated at the HF/6-31G level. Basis set superposition error (BSSE) corrections were determined in the gas phase at the HF/6-31G level, using the counterpoise correction method of Boys and Bernardi.[26] Zero-point energy (ZPE) corrections were included by scaling the ZPE correction given in the HF/6-31G level frequency calculation by the factor of 0.9135 given by Foresman and Frisch.[27] All calculations were carried out with the Gaussian 98 program.[28] Binding energies were determined by comparing the BSSE- and ZPE-corrected energies of the separately optimized ligand and tryptophan analogue to the energy of the complex. Solvent effects were added to the gas-phase-optimized structures using the polarizable continuum model (PCM) self-consistent reaction field of Tomassi and co-workers[29] with ϵ(THF) = 7.6, ϵ(EtOH) = 24.3, and ϵ(H2O) = 78.5.

Electrostatic potential surfaces were created with Molekel, available at www.cscs.ch/molekel/.[30] The electrostatic potential for each structure was mapped onto a total electron density surface contour at 0.002 e/Å^3. These surfaces were color-coded so that red signifies a value less than or equal to the minimum in positive potential and blue signifies a value greater than or equal to the maximum in positive potential.

Table 1. Mutations Testing Cation−π Interactions at α149

	Trp	F-Trp	F_2-Trp	F_3-Trp
epibatidine[a]	0.83 ± 0.08[b]	4.8 ± 0.1	9.3 ± 0.5	18 ± 2
cation−π[c]	32.6	27.5	23.3	18.9

[a] EC_{50} (μM) ± standard error of the mean. Racemic epibatidine was used in these experiments. The receptor has a Leu9′Ser mutation in M2 of the β subunit. [b] Rescue of wild type by nonsense suppression. [c] Reference 10. Value reported is the negative of the calculated binding energy of a probe cation (Na^+) to the ring, in kcal/mol.

Results

Unnatural amino acids were incorporated into the nAChR using in vivo nonsense suppression methods, and mutant receptors were evaluated electrophysiologically.[2] The structures and electrostatic potential surfaces of the agonists are presented in Figure 2. For these cationic agonists, the surface is positive everywhere; red simply represents relatively less positive, and blue relatively more positive.

In studies of weak agonists and/or receptors with diminished binding capability, it is necessary to introduce another mutation that independently decreases EC_{50}. We accomplished this via a Leu-to-Ser mutation in the β subunit at a site known as 9′ in the M2 transmembrane region of the receptor.[31−33] This M2-β9′ residue is almost 50 Å from the binding site, and previous work has shown that a Leu9′Ser mutation lowers the EC_{50} by a factor of roughly 10 without altering trends in EC_{50} values.[13,34] Measurements of EC_{50} represent a functional assay; all mutant receptors reported here are fully functioning ligand-gated ion channels. It is important to appreciate that the EC_{50} value is not a binding constant, but a composite of equilibria for both binding and gating. As we have shown in previous studies of LGIC using the unnatural amino acid methodology,[1,2,12,13,25,34−36] subtle changes in residues that define the agonist binding site are best thought of as altering EC_{50} by altering agonist affinity rather than by influencing gating processes.

Epibatidine Binds with a Potent Cation−π Interaction at Trp α149. The possibility of a cation−π interaction between epibatidine and Trp α149 was evaluated using our previously developed strategy, the incorporation of a series of fluorinated Trp derivatives (5-F-Trp, 5,7-F_2-Trp, 5,6,7-F_3-Trp, and 4,5,6,7-F_4-Trp). The EC_{50} values for the wild-type and mutant receptors are shown in Table 1. Attempts to record dose−response

(24) Nowak, M. W.; Gallivan, J. P.; Silverman, S. K.; Labarca, C. G.; Dougherty, D. A.; Lester, H. A. *Methods Enzymol.* **1998**, *293*, 504−529.
(25) Li, L. T.; Zhong, W. G.; Zacharias, N.; Gibbs, C.; Lester, H. A.; Dougherty, D. A. *Chem. Biol.* **2001**, *8*, 47−58.
(26) Boys, S. F.; Bernardi, F. *Mol. Phys.* **1970**, *19*, 553−566.
(27) Foresman, J. B.; Frisch, E. *Exploring Chemistry with Electronic Structure Methods*; Gaussian, Inc.: Pittsburgh, PA, 1996.
(28) Frisch, M. J.; Trucks, G. W.; Schlegel, H. B.; Scuseria, G. E.; Robb, M. A.; Cheeseman, J. R.; Zakrzewski, V. G.; Montgomery, J. A., Jr.; Stratmann, R. E.; Burant, J. C.; Dapprich, S.; Millam, J. M.; Daniels, A. D.; Kudin, K. N.; Strain, M. C.; Farkas, O.; Tomasi, J.; Barone, V.; Cossi, M.; Cammi, R.; Mennucci, B.; Pomelli, C.; Adamo, C.; Clifford, S.; Ochterski, J.; Petersson, G. A.; Ayala, P. Y.; Cui, Q.; Morokuma, K.; Malick, D. K.; Rabuck, A. D.; Raghavachari, K.; Foresman, J. B.; Cioslowski, J.; Ortiz, J. V.; Stefanov, B. B.; Liu, G.; Liashenko, A.; Piskorz, P.; Komaromi, I.; Gomperts, R.; Martin, R. L.; Fox, D. J.; Keith, T.; Al-Laham, M. A.; Peng, C. Y.; Nanayakkara, A.; Gonzalez, C.; Challacombe, M.; Gill, P. M. W.; Johnson, B. G.; Chen, W.; Wong, M. W.; Andres, J. L.; Head-Gordon, M.; Replogle, E. S.; Pople, J. A. *Gaussian* 98; Gaussian, Inc.: Pittsburgh, PA, 1998.
(29) Cossi, M.; Barone, V.; Cammi, R.; Tomasi, J. *Chem. Phys. Lett.* **1996**, *255*, 327−335.
(30) Flükiger, P.; Lüthi, H. P.; Portmann, S.; Weber, J. *Molekel*; Swiss Center for Scientific Computing: Manno, Switzerland, 2000.
(31) Filatov, G. N.; White, M. M. *Mol. Pharmacol.* **1995**, *48*, 379−384.
(32) Revah, F.; Bertrand, D.; Galzi, J. L.; Devillers-Theiry, A.; Mulle, C. *Nature* **1991**, *353*, 846−849.
(33) Labarca, C.; Nowak, M. W.; Zhang, H.; Tang, L.; Deshpande, P.; Lester, H. A. *Nature* **1995**, *376*, 514−516.
(34) Kearney, P. C.; Nowak, M. W.; Zhong, W.; Silverman, S. K.; Lester, H. A.; Dougherty, D. A. *Mol. Pharmacol.* **1996**, *50*, 1401−1412.
(35) Mu, T. W.; Lester, H. A.; Dougherty, D. A. *J. Am. Chem. Soc.* **2003**, *125*, 6850−6851.
(36) Petersson, E. J.; Choi, A.; Dahan, D. S.; Lester, H. A.; Dougherty, D. A. *J. Am. Chem. Soc.* **2002**, *124*, 12662−12663.

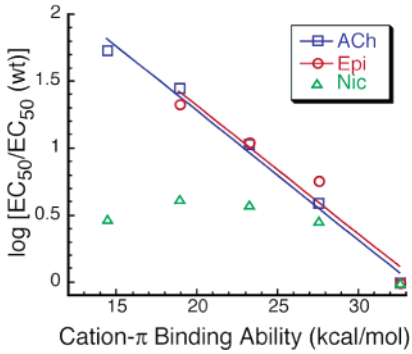

Figure 3. Fluorination plot for nAChR agonists. Epibatidine data are from Table 1, ACh data from ref 12, and nicotine data from ref 13. The log [EC_{50}/EC_{50}(wild type)] versus calculated cation−π ability is plotted for the series of fluorinated Trp derivatives at Trp α149. ACh data fit the line $y = 3.21 - 0.096x$, and epibatidine data fit the line $y = 3.23 - 0.096x$. The correlations for ACh and epibatidine fits were $R = 0.99$ and $R = 0.98$, respectively. Note that because the data for each agonist are normalized to the EC_{50} of the wild-type receptor, all three agonists share the point for the wild-type receptor, with coordinates (32.6, 0).

relations from 4,5,6,7-F_4-Trp at α149 were unsuccessful, because this mutant required epibatidine concentrations above 100 μM. At these concentrations, epibatidine becomes an effective open channel blocker,[19] confounding efforts to obtain an accurate dose−response curve. A clear trend can be seen in the data of Table 1: each additional fluorine produces an increase in EC_{50}.

As in previous work, our measure for the cation−π binding ability of the fluorinated Trp derivatives is the calculated binding energy of a generic probe cation (Na^+) to the corresponding substituted indole.[12,13,35] This method provides a convenient way to express the clear trend in the dose−response data in a quantitative way. A "fluorination plot" of the logarithmic ratio of the mutant EC_{50} to the wild-type EC_{50} versus the cation−π binding ability for Trp α149 reveals a compelling linear relationship (Figure 3). These data demonstrate that the secondary ammonium group of epibatidine makes a cation−π interaction with Trp α149 in the muscle-type nAChR.

Nicotine and Epibatidine Hydrogen Bond to the Carbonyl Oxygen of Trp α149. The recently reported crystal structure of AChBP with nicotine bound indicated a hydrogen bond between the pyrrolidine N^+−**H** of nicotine and the backbone carbonyl of Trp α149,[16] an interaction that had been anticipated by several modeling studies.[14,15] To evaluate this possibility, the backbone amide at this position was converted to an ester by replacing Thr α150 with the analogue α-hydroxythreonine (Tah) using the nonsense suppression methodology (Figure 4A). Converting an amide carbonyl to an ester carbonyl weakens the hydrogen-bonding ability of the oxygen. In studies of amide hydrogen bonds in the context of α-helices or β-sheets, the magnitude of the effect was 0.6−0.9 kcal/mol.[37,38]

The results of the incorporation of Tah at α150 are shown in Table 2. Upon ester substitution, the EC_{50} for nicotine increases 1.6-fold. The change is larger for the more potent agonist epibatidine; conversion of the backbone carbonyl of Trp α149 to an ester leads to a 3.7-fold increase in EC_{50} (Figure 4). In contrast, ACh, lacking a proton at the cationic center, shows a

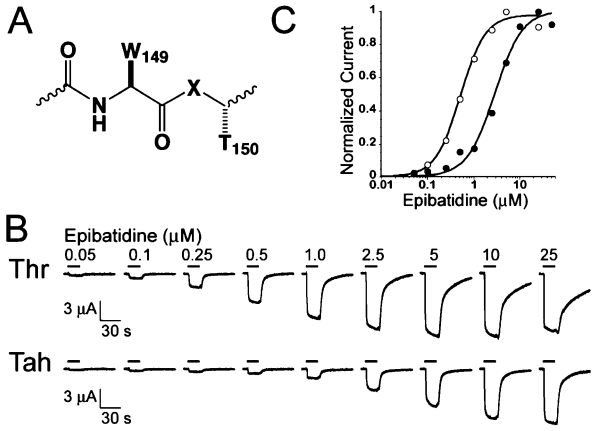

Figure 4. Hydrogen bond analysis of nAChR. (A) The backbone amide carbonyl of Trp α149 (X = NH) is replaced with an ester carbonyl (X = O) upon incorporation of Tah α150. (B, C) Electrophysiolgical analysis of epibatidine. (B) Representative voltage clamp current traces for oocytes expressing nAChRs suppressed with Thr or Tah at α150. Bars represent application of epibatidine at the concentrations noted. (**C**) Representative epibatidine dose−response relations and fits to the Hill equation for nAChR suppressed with Thr (○) and Tah (●). Studies incorporate a βLeu9′Ser mutation.

Table 2. Mutations Testing H-Bond Interactions at α150[a]

agonist	Thr[b]	Tah	Tah/Thr
ACh	0.83 ± 0.04	0.25 ± 0.01	0.30
nicotine	57 ± 2	92 ± 4	1.6
epibatidine	0.60 ± 0.04	2.2 ± 0.2	3.7

[a] EC_{50} (μM) ± standard error of the mean. The receptor has a Leu9′Ser mutation in M2 of the β subunit. [b] Rescue of wild type by nonsense suppression.

3.3-fold *decrease* in EC_{50}. These results further highlight the distinction between nicotinic and cholinergic agonists.

Computational Modeling. To further probe the interactions of drugs with Trp α149, a simple computational model was investigated. Considering only the interactions with Trp α149, we docked the ligands using ab initio (HF/6-31G) calculations, taking into account both the cation−π interaction and the carbonyl hydrogen bond. Initial tryptophan and ligand coordinates were taken from the AChBP-based homology models of Changeux.[15] Geometry optimizations, counterpoise corrections, and zero-point energy corrections were all performed in the gas phase. The optimized geometries for free ACh and nicotine are in keeping with previous calculations at higher levels of theory and with solution NMR studies, in that bent "tg" structures are favored for ACh and the trans form is favored for protonated nicotine.[39−41] The calculated binding energies are consistent with those from previous computational studies of metal-binding complexes with both cation−π and cation−carbonyl interactions[42−46] and studies of hydrogen bonds to protonated nicotine.[47,48]

(37) Deechongkit, S.; Nguyen, H.; Powers, E. T.; Dawson, P. E.; Gruebele, M.; Kelly, J. W. *Nature* **2004**, *430*, 101−105.
(38) Koh, J. T.; Cornish, V. W.; Schultz, P. G. *Biochemistry* **1997**, *36*, 11314−11322.
(39) Elmore, D. E.; Dougherty, D. A. *J. Org. Chem.* **2000**, *65*, 742−747.
(40) Vistoli, G.; Pedretti, A.; Villa, L.; Testa, B. *J. Am. Chem. Soc.* **2002**, *124*, 7472−7480.
(41) Partington, P.; Feeney, J.; Burgen, A. S. *Mol. Pharmacol.* **1972**, *8*, 269−277.
(42) Biot, C.; Buisine, E.; Rooman, M. *J. Am. Chem. Soc.* **2003**, *125*, 13988−13994.
(43) Biot, C.; Wintjens, R.; Rooman, M. *J. Am. Chem. Soc.* **2004**, *126*, 6220−6221.
(44) Sponer, J. E.; Sychrovsky, V.; Hobza, P.; Sponer, J. *Phys. Chem. Chem. Phys.* **2004**, *6*, 2772−2780.
(45) Sponer, J.; Leszczynski, J.; Hobza, P. *Biopolymers* **2001**, *61*, 3−31.
(46) Siu, F. M.; Ma, N. L.; Tsang, C. W. *Chem. Eur. J.* **2004**, *10*, 1966−1976.

Table 3. Solvent Effects on Binding Energy Differences[a]

	ester binding energy – amide binding energy (kcal/mol)			
agonist	gas	THF	ethanol	water
ACh	5.0	0.6	−1.7	−2.0
nicotine	6.1	3.1	1.2	−0.8
epibatidine[b]	8.0	7.0	5.0	4.7

[a] ϵ(THF) = 7.6, ϵ(ethanol) = 24.3, ϵ(water) = 78.5. [b] Average of energies for Epi enantiomers.

The calculated binding energies are summarized in Table 3 and in the Supporting Information. As expected, conversion of the Trp α149 amide to an ester weakens the binding interactions to both epibatidine and nicotine, and the calculated energetic consequence of ester conversion is larger for epibatidine than for nicotine (8 kcal/mol vs 6 kcal/mol). Using the PCM solvation model,[29] we also studied these interactions in solvents of differing polarity (Table 3). In each solvent, epibatidine favors amide binding over ester binding to a greater degree than nicotine. The changes in hydrogen-bonding energies observed in different solvent systems are consistent with similar calculations published by Houk and co-workers.[49]

The geometries shown in Figure 5 are consistent with the experimental trends observed. The cation−π interaction is expected to be much stronger for epibatidine than for nicotine. The calculated N^+ to π-centroid distance is substantially shorter for epibatidine (**a** in Figure 5). In addition, epibatidine points an N^+−**H** cationic center toward the Trp indole ring, vs the N^+CH_2−**H** of nicotine (Figure 5). The cationic center of epibatidine has a much more positive electrostatic potential than that of nicotine (+139 kcal/mol for epibatidine, +112 for nicotine). These potentials, indicators of cation−π binding strength, and the geometrical factors noted are consistent with the experimental observation that epibatidine has a much stronger cation−π interaction than nicotine.

Nicotine and epibatidine also make significant hydrogen bonds to the Trp α149 carbonyl oxygen with an N^+−**H** group (**b** in Figure 5). The geometrical parameters for interaction **b** with the two agonists are very similar, suggesting the two hydrogen bonds are comparably strong. In addition, the calculations suggest a second, previously unanticipated interaction between the $C_{aromatic}$−**H** of the carbon adjacent to the pyridine N of epibatidine and the same carbonyl (**c** in Figure 5). This type of C−H···O═C hydrogen bond has been seen in many protein structures and other systems, and the geometrical parameters of the epibatidine structures are compatible with previous examples.[50,51] (+)-Epibatidine has a calculated C−O distance (**c** in Figure 5) of 3.19 Å and a C−H−O angle of 151°; (−)-epibatidine has a longer C−O distance of 3.26 Å but a more favorable angle, 169°. In the computed nicotine-bound structure, the analogous distances and angles are less favorable (**c** in Figure 5), 3.42 Å and 139°, and the interaction is completely absent in the X-ray structure.

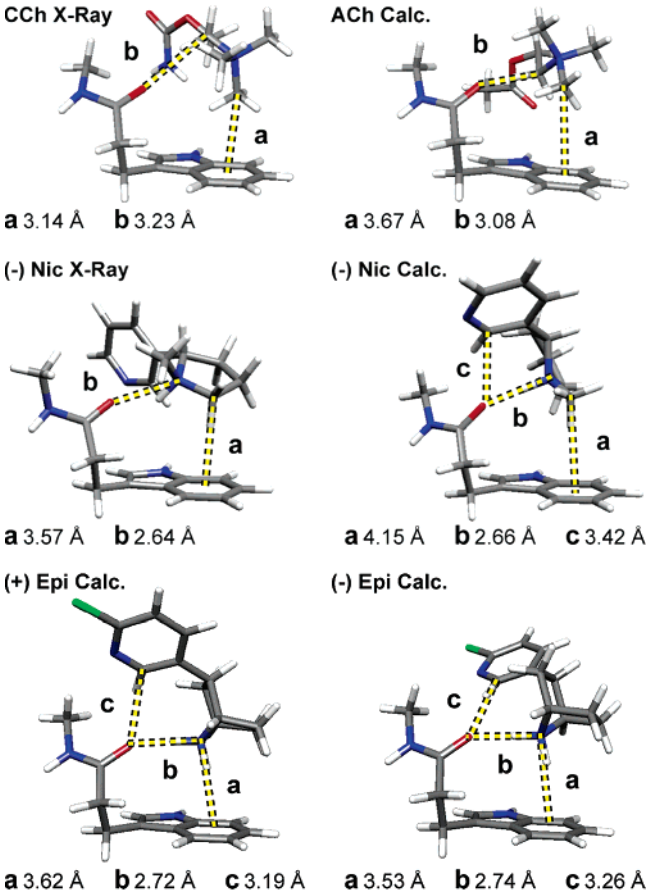

Figure 5. Crystal structure data (X-ray) and computational modeling (Calc.) of agonist binding. Crystal structures for CCh and nicotine were taken from Celie et al. (PDB ID 1UW6 (nicotine) and 1UV6 (CCh)).[16] Calculations were performed for ACh, (−)-nicotine, (+)-epibatidine, and (−)-epibatidine. Distance **a** represents a cation−π interaction, **b** represents an N^+−**H** or N^+C−**H** hydrogen bond with the backbone carbonyl, and **c** represents a $C_{aromatic}$−**H**···O═C hydrogen bond with the backbone carbonyl. Gas-phase HF/6-31G optimized geometries (Å) are reported. Hydrogens were added to the X-ray structures using Gaussview.

Discussion

A number of studies have identified key interactions that lead to the binding of small molecules at the agonist-binding site of nAChRs.[52] The field was dramatically altered with the appearance of the crystal structure of the ACh-binding protein. AChBP is not the nAChR, however. It is a small, soluble protein secreted from the glial cells of a snail, and it is <25% identical to its closest relative in the nAChR family, α7.[8] It remains to be established just how relevant AChBP is to the functional receptors.[53] The methodology of incorporating unnatural amino acids into these receptors provides a functional tool to address this task.

Previously, we observed an intriguing result: nicotine and ACh use different noncovalent interactions to bind the muscle-type nAChR.[13] ACh forms a strong cation−π interaction with Trp α149; nicotine does not. Although it is known as the nicotinic receptor, the form we study here, that found in the peripheral nervous system, is relatively insensitive to nicotine. At this muscle-type receptor, ACh is over 70-fold more potent than nicotine. The behavioral and addictive effects of nicotine

(47) Graton, J.; Berthelot, M.; Gal, J. F.; Laurence, C.; Lebreton, J.; Le Questel, J. Y.; Maria, P. C.; Richard, R. *J. Org. Chem.* **2003**, *68*, 8208−8221.
(48) Graton, J.; van Mourik, T.; Price, S. L. *J. Am. Chem. Soc.* **2003**, *125*, 5988−5997.
(49) Cannizzaro, C. E.; Houk, K. N. *J. Am. Chem. Soc.* **2002**, *124*, 7163−7169.
(50) Thomas, K. A.; Smith, G. M.; Thomas, T. B.; Feldmann, R. J. *Proc. Natl. Acad. Sci. U.S.A.* **1982**, *79*, 4843−4847.
(51) Duan, G.; Smith, V. H.; Weaver, D. F. *J. Phys. Chem. A* **2000**, *104*, 4521−4532.
(52) Schmitt, J. D. *Curr. Med. Chem.* **2000**, *7*, 749−800.
(53) Bouzat, C.; Gumilar, F.; Spitzmaul, G.; Wang, H. L.; Rayes, D.; Hansen, S. B.; Taylor, P.; Sine, S. M. *Nature* **2004**, *430*, 896−900.

arise exclusively from interactions with one or more neuronal subtypes of nAChR found in the central nervous system, where nicotine and ACh are generally comparably potent. We therefore wanted to probe a nicotinic-type agonist that is potent at the muscle receptor, and epibatidine was the logical choice. This alkaloid natural product possesses potent analgesic properties[54] and has served as a lead compound for a number of pharmaceutical programs targeted at the nAChR.[21] In the present work, we find two specific interactions that distinguish among the three agonists considered here, ACh, nicotine, and epibatidine.

First, we now find that epibatidine makes a strong cation$-\pi$ interaction with Trp α149 of the muscle-type nAChR. This result contrasts sharply to that for nicotine, and this observation helps to explain the much higher affinity of epibatidine for this receptor relative to nicotine. The apparent magnitudes of the cation$-\pi$ interactions, indicated by the slopes of the fluorination plots in Figure 3, are comparable for ACh and epibatidine. This similarity is somewhat surprising. It is well established that quaternary ammonium cations make weaker cation$-\pi$ interactions than protonated ammoniums (be they primary, secondary, or tertiary), and the electrostatic model of the cation$-\pi$ interaction nicely rationalizes this effect.[9,10,55] In addition, we have shown that, when serotonin is the agonist binding to a Trp in two different receptors, a steeper slope for the fluorination plot is seen than that for ACh in the nAChR.[13,35] Serotonin contains a primary ammonium ion, and so the steeper slope is considered to be consistent with the expected stronger cation$-\pi$ interaction. We conclude that epibatidine makes a strong cation$-\pi$ interaction—comparable to that for ACh—but that, at least at the muscle receptor, it cannot maximize its binding to the indole ring of Trp α149 due to other binding constraints.

The second discriminator we have probed is hydrogen bonding. A newer crystal structure of the AChBP includes nicotine at the binding site.[16] The structure confirms the existence of a hydrogen bond between nicotine and the backbone carbonyl of Trp α149, an interaction anticipated by modeling studies. In efforts to probe this noncovalent interaction, we studied the effects of decreasing the hydrogen bond acceptor ability of the backbone carbonyl of Trp α149. In such studies, the clear distinction between ACh and nicotinic agonists is strengthened. Nicotine and epibatidine, containing a tertiary and secondary cationic center, respectively, both show increases in EC_{50} compared to the native receptor in response to the amide-to-ester modification (Table 2). The effect is larger with the more potent agonist, epibatidine. Thus, the experimental data support the suggestion that nicotine and epibatidine interact with the nAChR through a hydrogen bond with the backbone carbonyl of Trp α149.

ACh, with a quaternary cationic center that cannot make a conventional hydrogen bond, shows a decrease in EC_{50} at the ester-containing receptor compared to the native receptor. We had anticipated that the binding of ACh would be unaffected by such a subtle change. The origin of this effect is unclear at present and is the object of further investigation. Here we consider two possibilities.

In the recently reported crystal structure of AChBP binding to carbamylcholine (CCh),[16] a cholinergic analogue of ACh, the backbone carbonyl oxygen of interest here makes contact with a CH_2 group adjacent to the $N^+(CH_3)_3$ group (CCh = $NH_2C(O)OCH_2\mathbf{CH_2}N^+(CH_3)_3$). This CH_2 carries a significant positive charge, like the CH_3 groups, and so a favorable electrostatic interaction is possible. This interaction with CCh would be much weaker than the $N^+-\mathbf{H}$ hydrogen bonds of nicotine and epibatidine, but perhaps not negligible. Interestingly, Sixma and co-workers noted that the binding of CCh to AChBP is less enthalpically favorable than that of nicotine. They attribute this observation to the net unfavorable burial of the carbonyl oxygen by CCh. The weak interaction with the CH_2 group cannot compensate for the loss of hydrogen bonding, presumably to water molecules. This desolvation penalty would be less severe with a backbone ester than with an amide, so ACh binds more favorably to the ester-containing receptor.

We also propose a second possible explanation. Highly conserved Asp α89 (Asp 85 in AChBP numbering) makes a number of significant contacts with nearby residues, suggesting that it plays a key structural role in shaping the agonist binding site.[8,16] One such interaction is a hydrogen bond between the Asp α89 carboxylate side chain and the NH group of the backbone amide of Trp α149. The amide-to-ester mutation of the present study eliminates the NH and so removes this interaction. A possible outcome of this alteration would be a structural change that would affect gating or ligand binding in a general way. Very recently, Lee and Sine have shown that mutating this residue to Asn slows the kinetics of ACh binding to the receptor.[56]

Regardless of its origin, it is reasonable to propose that the effect of ester substitution we see with ACh can be considered as the "background" for the Thr150Tah mutation. That is, if the magnitude of the cholinergic $N^+CH_2\cdots O{=}C$ interaction is small, then both the desolvation and gating effects proposed are "generic" and should occur with all agonists. In this case, the changes in EC_{50} we measure for nicotine or epibatidine actually represent the product of two terms: a generic 3.3-fold decrease evidenced by ACh, and a term specific to nicotine or epibatidine. As such, the drop in hydrogen-bonding strength is calculated to be 1.6 × 3.3, or ∼5-fold for nicotine, and 3.7 × 3.3, or ∼12-fold for epibatidine. Energetically, these factors correspond to 1.0 and 1.5 kcal/mol, respectively. This is the first experimental evaluation of a hydrogen-bonding interaction between a protein backbone and a ligand using backbone ester substitution. The magnitude we see is larger than what has been reported for amide···amide hydrogen bonds that stabilize protein secondary structure.[37,38] Context is always important in such effects, so it is not surprising to see a difference between a ligand···backbone interaction and a backbone···backbone interaction. In addition, the hydrogen bond donor in the present system is cationic, as opposed to the neutral amide NH in the secondary structure studies. Hydrogen bonding involving ionic species is often stronger than for neutral species, and so our values seem quite reasonable.

Our experimental studies suggested that the two structurally quite similar molecules, nicotine and epibatidine, bind differently to the nAChR. Epibatidine experiences both a cation$-\pi$ interaction and a backbone interaction with Trp α149, while nicotine experiences only the latter. In an effort to shed some light on this issue, we performed appropriately simple calcula-

(54) Spande, T. F.; Garraffo, H. M.; Edwards, M. W.; Yeh, H. J. C.; Pannell, L.; Daly, J. W. *J. Am. Chem. Soc.* **1992**, *114*, 3475−3478.
(55) Mecozzi, S.; West, A. P.; Dougherty, D. A. *J. Am. Chem. Soc.* **1996**, *118*, 2307−2308.
(56) Lee, W. Y.; Sine, S. M. *J. Gen. Physiol.* **2004**, *124*, 555−567.

tions in which we docked both drugs onto Trp α149. The goal here was not to obtain quantitative binding information. There are no doubt many other side chains that also contribute to the binding of these drugs, and, despite the AChBP structure, it is a substantial challenge to know how to evaluate these interactions. Our calculated ACh binding geometry in Figure 5 agrees surprisingly well with the CCh crystal structure. The calculated geometry for nicotine, however, deviates from both the X-ray structure of nicotine bound to AChBP[16] and the docked homology models of Changeux and co-workers.[15] The nicotine geometry in Figure 5 is obtained in HF/6-31G minimizations starting from either the docked coordinates of Le Novère et al. or the position of bound nicotine in the AChBP crystal structure. The fact that the relationship of nicotine to Trp α149 changes upon minimization implies that other side chains are necessary to hold nicotine in the crystal structure orientation. Nevertheless, because the goal of our computational studies was to supplement our experimental results, these simple gas-phase geometry optimizations are informative.

Remarkably, the relatively simple model calculations we have conducted afford trends that nicely parallel our experimental findings. One key test of the calculations arises from the fact that, experimentally, the EC_{50} values of (+)- and (−)-epibatidine are nearly identical for a given acetylcholine receptor subtype.[54] We find that the calculated binding energies to Trp α149 and the key geometrical parameters (Figure 5) are indeed very similar for the two enantiomers.

In the gas phase, it is better to bind to the backbone amide than the ester for all three agonists. However, as solvation is introduced, the trend is reversed (Table 3). Interestingly, when a solvent of moderate polarity—ethanol—is used, ACh prefers the ester backbone, while nicotine and epibatidine prefer the amide, just as we see in our experimental studies. The ethanol environment is defined in these calculations by a dielectric constant of 24.3. Two lines of evidence indicate that this is a reasonable estimate of the effective dielectric of the binding pocket of the AChBP or nAChR. First, it is consistent with previous experimental measurements of a perturbed local pK_a in the nAChR binding site.[36] Second, calculations of the solvent-accessible surface area (see Supporting Information) of the binding site residues show that Trp 149 is 11% solvent-accessible. A moderate dielectric of 24.3 seems reasonable for the partially exposed binding site. Thus, it may be, as discussed above, that the EC_{50} for ACh decreases when the ester is introduced because the desolvation penalty of the ester carbonyl oxygen is less severe than that of the amide.

The computer modeling summarized in Figure 5 also nicely rationalizes the observed cation−π binding behavior. Epibatidine, like ACh, makes much closer contact with the indole ring than does nicotine. Both the distance (**a** in Figure 5) and the electrostatic potential on the interacting hydrogen (Figure 2, N^+−**H** in epibatidine vs N^+CH_2−**H** in nicotine) suggest a more favorable cation−π interaction for epibatidine than for nicotine.

The larger amide/ester effect seen for epibatidine versus nicotine suggests a stronger N^+−**H**···O═C hydrogen bond in the former. However, in the docked structures these hydrogen bonds (**b** in Figure 5) are geometrically very similar for epibatidine and nicotine, suggesting that they are of comparable strengths. The docking studies do, however, suggest an alternative explanation. The docked epibatidine structure clearly shows a $C_{aromatic}$−**H**···O═C hydrogen bond from the drug to the backbone carbonyl. C−H···O hydrogen bonds are well known, if structural features create a significant partial positive charge on the hydrogen.[50,51] The $C_{aromatic}$−H hydrogen bond of interest should be highly polarized to favor a hydrogen bond, because it is ortho to a pyridine nitrogen and meta to a chlorine substituent. Geometrically, the $C_{aromatic}$−**H** hydrogen bond to the carbonyl (**c** in Figure 5) is tighter and better aligned for both epibatidine enantiomers than for nicotine. The computations thus suggest that it is this unconventional hydrogen bond (**c**), rather than the anticipated hydrogen bond (**b**), that rationalizes the slightly greater response of epibatidine versus nicotine to the backbone change. Note that the small structural differences between epibatidine and nicotine nicely rationalize their differing affinities. The secondary ammonium of epibatidine provides two N^+−**H**'s that can undergo strong electrostatic interactions—a cation−π interaction and a hydrogen bond to a carbonyl. The tertiary ammonium of nicotine allows a strong hydrogen bond, but not a significant cation−π interaction. Second, the slightly different positioning of the pyridine group in epibatidine allows for a more favorable $C_{aromatic}$−**H**···O═C hydrogen bond than for nicotine.

The ability to systematically modify receptor structure enables studies of drug−receptor interactions with unprecedented precision. In other work, we have established that a single drug, serotonin, can adopt two different binding orientations at highly homologous serotonin receptors.[35] Here we show that two agonists binding to the same binding site can make use of quite different noncovalent binding interactions to activate the receptor, even if the agonists are structurally very similar. No doubt medicinal chemists have anticipated such a result for some time, but it is only with the high-precision physical chemistry tools described here that such possibilities can be directly addressed.

In summary, a combination of unnatural amino acid mutagenesis and computer modeling has led to the following conclusions. The nicotinic agonists nicotine and epibatidine both experience a favorable hydrogen-bonding interaction with the carbonyl of Trp α149, which is qualitatively distinct from the interaction (if any) of ACh with this group. The greater potency of epibatidine arises from the fact that, along with hydrogen bonding, epibatidine experiences a cation−π interaction comparable to that seen with ACh. In addition, epibatidine picks up a subtle $C_{aromatic}$−**H**···O═C hydrogen bond that nicotine does not.

At the neuronal nAChR, both epibatidine and nicotine show much higher affinities than at the muscle type studied here, although epibatidine remains the more potent agonist across all receptor types. This suggests that the differentiating cation−π interaction seen here may carry over to the more pharmacologically relevant neuronal receptors. Additional studies along these lines are underway.

Acknowledgment. We thank the NIH (NS 34407 and NS 11756) for support of this work, and Professor George Petersson for assistance.

Supporting Information Available: Synthetic procedures, discussion of the nAChR binding site dielectric constant, and HF/6-31G optimized geometries. This material is available free of charge via the Internet at http://pubs.acs.org.

JA0461771